FEMS Yeast Research, 16, 2016, fow063

doi: 10.1093/femsyr/fow063
Advance Access Publication Date: 3 August 2016
Research Article

RESEARCH ARTICLE

Differential hypersaline stress response in *Zygosaccharomyces rouxii* complex yeasts: a physiological and transcriptional study

Lisa Solieri[1,*], Veronica Vezzani[1], Stefano Cassanelli[1], Tikam Chand Dakal[1], Jacopo Pazzini[2,3] and Paolo Giudici[1]

[1]Department of Life Sciences, University of Modena and Reggio Emilia, via Amandola 2, Besta building, I-42124 Reggio Emilia, Italy, [2]Department of Physics "G. Galilei", University of Padova, and INFN, via Marzolo 8, I-35131 Padova, Italy and [3]CERN, European Organization for Nuclear Research, CH-1211 Geneva 23, Switzerland

*Corresponding author: Department of Life Sciences, University of Modena and Reggio Emilia, via Amandola 2, Besta building, 42124 Reggio Emilia, Italy. Tel: +39-(0)522-522057; E-mail: lisa.solieri@unimore.it

One sentence summary: The high salinity response in *Zygosaccharomyces rouxii* complex yeasts was studied by analysing how growth kinetic parameters are affected by transcriptional regulation of Na^+/H^+ antiporter-encoding *ZrSOD* genes and metabolically compatible osmolyte accumulation.

Editor: Isak Pretorius

ABSTRACT

The *Zygosaccharomyces rouxii* complex comprises three distinct lineages of halotolerant yeasts relevant in food processing and spoilage, such as *Z. sapae*, *Z. rouxii* and a mosaic group of allodiploid strains. They manifest plastic genome architecture (variation in karyotype, ploidy level and Na^+/H^+ antiporter-encoding gene copy number), and exhibit diverse tolerances to salt concentrations. Here, we investigated accumulation of compatible osmolytes and transcriptional regulation of Na^+/H^+ antiporter-encoding *ZrSOD* genes during salt exposure in strains representative for the lineages, namely *Z. sapae* ABT301^T (low salt tolerant), *Z. rouxii* CBS 732^T (middle salt tolerant) and allodiploid strain ATCC 42981 (high salt tolerant). Growth curve modelling in 2 M NaCl-containing media supplemented with or without yeast extract as nitrogen source indicates that moderate salt tolerance of CBS 732^T mainly depends on nitrogen availability rather than intrinsic inhibitory effects of salt. All the strains produce glycerol and not mannitol under salt stress and use two different glycerol balance strategies. ATCC 42981 produces comparatively more glycerol than *Z. sapae* and *Z. rouxii* under standard growth conditions and better retains it intracellularly under salt injuries. Conversely, *Z. sapae* and *Z. rouxii* enhance glycerol production under salt stress and intracellularly retain glycerol less efficiently than ATCC 42981. Expression analysis shows that, in diploid *Z. sapae* and allodiploid ATCC 42981, transcription of gene variants *ZrSOD2-22*/*ZrSOD2* and *ZrSOD22* is constitutive and salt unresponsive.

Keywords: *Zygosaccharomyces* yeasts; salt; stress response; glycerol; Na^+/H^+ antiporters; transcription analysis

INTRODUCTION

High concentrations of external ionic solutes (mainly Na^+) reduce water activity (a_w) and limit yeast growth in natural and industrial environments. Hypersaline stress harms cell wall and plasma membrane, increases intracellular ion toxicity, changes osmotic pressure and shrinks cell volume. Given that sodium ions are abundant in natural environments, yeasts, like other unicellular microorganisms, have evolved different strategies to maintain a relatively low intracellular concentration of Na^+ cations under salt injuries (Ruiz and Ariño 2007). Despite their

Received: 10 June 2016; **Accepted:** 31 July 2016

diversity, these mechanisms basically rely on morphological and structural modifications of the cell wall and plasma membrane; modulation of alkali metal cation transport systems; and production, accumulation and retention of metabolically compatible osmolytes (De Nadal, Ammerer and Posas 2011).

Halotolerance, i.e. the capability to adapt to high concentrations of ionic solutes, is a very desirable trait necessary for several yeast-driven industrial biotransformations (Dakal, Solieri and Giudici 2014), and makes halotolerant yeasts more attractive than the moderately salt-tolerant *Saccharomyces cerevisiae* as biocatalysts. *Zygosaccharomyces rouxii* and related species (referred to as *Z. rouxii* species complex) are the halotolerant yeasts most phylogenetically related to *S. cerevisiae* and have a relevant role in food industry (Solieri *et al.* 2013). This group comprises three taxonomic lineages, such as the haploid *Z. rouxii* species, the diploid sister species *Z. sapae* and a pool of allodiploid/aneuploid mosaic strains with uncertain taxonomic position. The diploid species *Z. sapae* is mainly found during alcoholic fermentation of traditional balsamic vinegar (TBV) and other sugary condiments (Solieri and Giudici 2008; Solieri *et al.* 2008; Solieri, Dakal and Giudici 2013), whereas the haploid *Z. rouxii* and the allodiploid/aneuploidy strains of the mosaic lineage are associated with fermentative elaboration of miso and soy sauce (Solieri and Giudici 2008; Suezawa, Suzuki and Mori 2008; Solieri *et al.* 2013). *Zygosaccharomyces rouxii* complex yeasts can also spoil sugary and salty foodstuffs to the detrimental of their quality and security (Stratford 2006; Fleet 2011). All these yeasts exhibit the same ability to withstand sugar concentrations up to 60%–70% ($a_w \leq 0.88$; osmotolerance), whereas display variable tolerance to 16%–25% (w/v) NaCl amounts (corresponding to 0.92–0.85 a_w range) (Dakal, Solieri and Giudici 2014). We previously demonstrated that *Z. sapae* ABT301^T shows less adaptation to salt stress, whereas strains belonging to mosaic lineage, such as allodiploid ATCC 42981, and aneuploids CBS 4837 and CBS 4838, grow faster in rich medium and exhibit strong adaptation to suboptimal growth conditions (Solieri, Dakal and Bicciato 2014). By contrast, *Z. rouxii* CBS 732^T displays intermediate growth ability both in basal and salt-stress growth conditions (Bubnová, Zemančíková and Sychrová 2014; Solieri, Dakal and Bicciato 2014).

Since salt tolerance has different levels in this clade, *Z. rouxii* complex is a very promising model for elucidating cellular mechanisms underlying salt adaptation in yeast. However, several questions about the strain and species-specific differences in halotolerance remain poorly understood. Previous efforts to elucidate these mechanisms were mainly limited to strain ATCC 42981 that was supposed to be a recently formed allodiploid between *Z. rouxii* and another unrecognised species (named *Z. pseudorouxii*) (James *et al.* 2005; Gordon and Wolfe 2008). Differently from haploid *Z. rouxii* (Kinclová, Potier and Sychrová 2001), ATCC 42981 experienced expansion of gene repertoires involved in alkali metal cation transports (Watanabe, Miwa and Tamai 1995; Iwaki *et al.* 1998), glycerol biosynthesis (Iwaki *et al.* 2001; Watanabe, Tsuchimoto and Tamai 2004) and high osmolarity glycerol (HOG) regulatory pathway (Iwaki, Tamai and Watanabe 1999; Iwaki *et al.* 2001). In particular, ATCC 42981 genome harbours two Na^+/H^+ antiporter genes, namely *ZrSOD2* and *ZrSOD22*, which selectively mediate the Na^+ ions extrusion. ZrSod2 antiporter exhibits 99.6% identity at the amino acid level with the ZrSod2-22 variant found in *Z. rouxii* (Kinclová, Potier and Sychrová 2001, 2002), whereas ZrSod22 is slightly divergent (83.7% identity), with major number of aa substitutions and indels being localised in the hydrophilic C-terminus, which is involved in Na^+ ion detoxification (Kinclová-Zimmermannova and Sychrová 2006). Like ATCC 42981, *Z. sapae* ABT301^T also possesses two gene variants encoding Na^+/H^+ antiporters, namely *ZrSOD2-22* and *ZrSOD22*, but it is less salt tolerant than ATCC 42981 (Solieri *et al.* 2008). Therefore, copy number variation and polymorphisms in these genes have no obvious correlation with variation in saline tolerance (Watanabe, Miwa and Tamai 1995; Iwaki *et al.* 1998).

In this study, we investigate *Z. rouxii* CBS 732^T, *Z. sapae* ABT301^T and allodiploid ATCC 42981 for two main cellular modifications elicited by salt stress, i.e. (1) the production and intracellular retention of metabolically compatible osmolytes having role in balancing osmotic pressure and counteracting cell shrinking; (2) the transcriptional regulation of ion transport systems, which mediate Na^+ extrusion and protect the cell from intracellular pH imbalance, dissipation of plasma membrane potential and toxic effects of Na^+ cations. In order to understand regulation of ion transport system at transcription level, two novel sets of PCR primers were designed for targeting different *ZrSOD* copy variants by RT-qPCR assays.

MATERIALS AND METHODS

Yeast strains, media and culture conditions

The yeasts analysed in this work were three *Zygosaccharomyces* strains associated with various food processes (Table 1). *Zygosaccharomyces rouxii* CBS 732^T was retrieved from Yeast Collection of the Centraalbureau voor Schimmelcultures (CBS; Utrecht, the Netherlands), whereas ATCC 42981 strain was an allopolyploid yeast from the American Type Culture Collection (ATCC; Manassas, VA). *Zygosaccharomyces sapae* was isolated from TBV (Solieri *et al.* 2013) and deposited in the Unimore Microbial Culture Collection (www.umcc.unimore.it). All strains were routinely grown at 26°C in YPD medium containing 1% yeast extract (YE) (Difco Laboratories, Detroit, MI), 1% Bacto peptone (Difco) and 2% glucose, supplemented or not with 1.5% agar. Pure cultures were

Table 1. Strains used in this study and their main characteristics.

Strains	Taxonomy	Other collections	Source	Mating-type/ thallism	Spore	Ploidy ratio	*ZrSOD* gene variants
CBS 732^T	*Zygosaccharomyces rouxii*	NCYC 568, NRRL Y-229	Grape must	*MATα*/homothallic	+	1.3	*ZrSOD2-22*
ATCC 42981	Mosaic lineage	–	Miso	**A**α	–	2.1	*SOD2*; *SOD22*
ABT301^T	*Zygosaccharomyces sapae*	UMCC 152, CBS 12607, MUCL54092	TBV	**A**$\alpha\alpha\alpha$	w	2.0	*SOD2-22*; *SOD22*
NCYC 3042	*Zygosaccharomyces pseudorouxii*	–	soft drink	Nd	nd	nd	*SOD22*

TBV, traditional balsamic vinegar; w, weak ability to sporulate; -, not available; nd, not determined.

maintained at 4°C on YPD slants for the duration of experiments, and the stocks were stored at –80°C with glycerol at final concentration of 25% (v/v) for long-term preservation.

For growth tests, RNA extraction and polyol determination, we used synthetic medium [5% glucose and 6.7 g/L Yeast Nitrogen Base (YNB; Difco)] supplied with 2.0 M NaCl (NaCl-SM) (Solieri, Dakal and Bicciato 2014) and with 2.0 M NaCl plus 1% (w/v) yeast extract (NaCl-YESM), respectively. The corresponding media without salt (SM and YESM, respectively) were used as control conditions.

Growth assay and mathematical modelling

Strains were precultured in YPD medium for 24 h at 28°C and used to inoculate, each in three replicates, four sets of baffled Erlenmeyer flasks containing 70 ml of SM, YE-SM, NaCl-SM and NaCl-YESM media, respectively, at the final concentration of 5×10^6 CFU/ml. Cells were cultured at 28°C under shaking conditions (150 rpm) and cell growth was monitored as optical density change at 600 nm (OD_{600}) at least two times a day until reaching the late-stationary phase (no change in OD measurement detected in at least three consecutive readings). For each growth assay, length of lag phase (λ), growth rate (maximum slope μ) and the maximum cell growth (A) were computed with the parametric fitting models logistic, Gompertz and Richards.

Analytical determination

Intra- and extracellular glycerol and mannitol concentrations were determined by enzymatic kits (Megazyme), according to the manufacturer's instructions. Intra- and extracellular fractions were obtained as previously reported (Watanabe, Tsuchimoto and Tamai 2004). Briefly, 1 ml of unstressed and salt-stressed yeast cultures grown to exponential (L) (OD_{600} ranged from 0.6 to 1.2) and stationary (S) phases were centrifuged at 10000 rpm for 5 min at 4°C. The supernatant representing extracellular fraction was stored at –20°C for further enzymatic analysis. Cell extracts were prepared as follows. The cell pellets were resuspended in fresh medium and submitted to mechanical lysis at the maximum speed by using glass beads (0.22 μm diameter) for 4 min followed by a boiling step for 5 min. The homogenate was centrifuged at 10 000 rpm for 10 min at 4°C, and the resulting supernatant fluid was used as intracellular fraction.

RNA extraction, cDNA synthesis and qualitative RT-PCR

Total RNA was extracted from 2×10^8 CFU of L- and S-grown cells grown in standard and salt-stress conditions using the ZR Fungal/Bacterial RNA MicroPrep Kit (ZymoReasearch, Irvine, CA, USA), as previously reported (Bizzarri et al. 2016). RNA concentrations and purity were determined using a Nanodrop spectrophotometer ND-1000 (Nanodrop Technologies, Wilmington, DE), whereas RNA integrity was determined by electrophoresis in 1% (w/v) agarose gel. Single-strand cDNA synthesis was carried out in a final volume of 40 μl containing 400 U of RevertAid H Minus Reverse Transcriptase (Thermo Scientific, Waltham, USA), 1X Reaction Buffer, 40 U of RiboLock RNase Inhibitor, 1 mM dNTPs Mix, 0.5 μM Oligo$(dT)_{18}$ primer and 1 μg RNA template. Reverse transcription reactions were performed at 42°C for 60 min and the reverse transcriptase was inactivated by heating at 72°C for 10 min.

Qualitative RT-PCR analysis was performed on *SOD2-22*/*SOD2* and *SOD22* gene variants by using the primer pairs SOD1F/SOD1R and SOD2F/SOD2R, respectively (James et al. 2005). cDNA template (25 ng) was amplified in a final volume of 20 μl containing 1X PCR Buffer, 0.5 U rTaq DNA polymerase (Takara Bio Inc., Japan), 200 μM of each dNTP (2.5 mM each) and 0.3 μM of each primer. RT-PCR reactions were carried out with three biological replicates and included genomic DNA (gDNA) templates as positive controls and non-reverse-transcribed RNA templates (-RT controls) to test contamination with gDNA. Successful amplification was checked by electrophoresis in 2% (w/v) agarose gel (0.5X TBE). Cycling conditions were 94°C for 5 min, followed by 35 cycles of denaturation step at 94°C for 30 s, an annealing step at 55°C for 45 s and an extension step at 72°C for 1.5 min. When required, *SOD2-22*, *SOD2* and *SOD22* amplicons were confirmed by sequencing, as reported by Solieri et al. (2008).

Quantitative RT-PCR (RT-qPCR)

Oligonucleotide primer pairs SOD2-22˙1F (5′-CATGACGTGTACCATGTTGA-3′)/SOD 2–22_1R (5′-CCTGCTCTCTCAGAAGTTTG-3′) and SOD22_F4 (5′-GTTCCACAAGGAGGGACTTG-3′)/SOD22_R4 (5′-ACGAGCTTCGTTGGTGATCT-3′) were designed to selectively amplify *SOD2-22*/*SOD2* and *SOD22* gene variants, respectively, in SYBR Green-based RT-qPCR assays. CBS 732^T *SOD2-22* (AJ252273), ATCC 42981 *SOD22* (AB010106) and ATCC 42981 *SOD2* (D43629) gene sequences were aligned with Clustal Omega (Goujon et al. 2010) and used as templates for primer design. The criteria adopted for designing the primers were the following: amplicon length between 95 and 300 bp, primer length between 18 and 24 nt an optimal GC content of 50%–60% with a melting temperature (T_m) of 60°C. For each qPCR primer set, the PCR efficiency was predicted using the open source tool Primer Efficiency (http://srvgen.upct.es/index.html) (Mallona, Weiss and Marcos 2011). Primer set specificity and effectiveness were validated by checking the presence and the approximate size of qPCR products using gDNAs from ATCC 42981, $ABT301^T$, CBS 732^T and NCYC 3042 as templates. *SOD22* full-length products were PCR amplified from ATCC 42981 according to Kinclová, Potier and Sychrová (2001), gel-purified using Gene JET Gel Extraction Kit (Thermo Scientific, Waltham, MA, USA) and used as template in semi-nested PCR reactions using internal qPCR primer sets. The qPCR reaction was performed on an Applied Biosystems 7300 Real-Time PCR instrument (Applied Biosystems, Foster City, CA, USA). Reactions contained 12.5 μl of MaximaTM SYBR Green/ROX qPCR Master Mix (Fermentas, Waltham, MA, USA), 0.3 μM of each primer, 5 μl of diluted cDNA template (six standard dilution points in a concentration range of 10–0.02 ng/μl) and ultrapure water to a reaction volume of 25 μl. Cycling protocol included an initial denaturation at 95°C for 10 min and 40 cycles of denaturation at 95°C for 15 s, annealing at 60°C for 30 s and extension at 72°C for 40 s, followed by the melt curve analysis to check the presence of unspecific amplicons and primer dimers. Each RT-qPCR reaction set included water as a negative no-template control instead of cDNA. Amplification profiles, baselines and thresholds were analysed with 7300 SDS 1.4 Software (Applied Biosystems). Relative mRNA expression of target genes was normalised by comparative Ct method ($2^{-\Delta\Delta Ct}$, $\Delta Ct = Ct_{target}\text{-}Ct_{reference}$, $\Delta\Delta Ct = \Delta Ct_{salt}\text{-}\Delta Ct_{standard}$) (Livak and Schmittgen 2001), using the *Z. rouxii* housekeeping gene *ACT1* (*ZrACT1*; XM˙002497273) as reference gene (Bizzarri et al. 2016). Amplification efficiencies were derived from the amplification plots using the program LinRegPCR when the low gene expression level did not provide enough dynamic range to build a reliable standard curve. Differentially expressed genes were defined

as at least 2-fold up- or downregulated in the stress compared to control conditions.

Statistical analysis

All statistical tests and parametric fitting models were computed with GraphPad Prism 5 (GraphPad Software, La Jolla, CA, USA). The Akaike Information Criterion (AIC) was used to select the best-fitting model. The compatibility of the growth parameters (λ, μ and A) extracted from the fit under different conditions or between strains under the same environmental condition was tested by estimating the level of agreement of their difference with zero, considered as the null hypothesis in the tests, under the assumption of independent measurements. Two parameters were considered to be significantly different if their uncertainty-normalised difference, $|\sigma|$, is found to be greater than 3, corresponding to a probability to reject the null hypothesis $> 99.7\%$ under the assumption of Gaussian distribution for the outcome of the fit parameters.

The effects of strains, salt treatment and their interaction on glycerol and mannitol amounts were analysed by two-way ANOVA and Tukey's *post hoc* multiple comparison test. Paired Student's t test (two tailed) was used to compare total glycerol production (sum of intra- and extracellular amounts) and target gene expression between unstressed and salt-stressed conditions. For all the analyses, a P-value cut-off of 0.05 was used.

RESULTS AND DISCUSSION

Preliminary evaluation of growth media

High salt stress has multiple effects on yeast cell physiology, metabolism and growth. To understand how hyperosmotic stress impacts growth capability of *Zygosaccharomyces rouxii*, *Z. sapae* and allodiploid strain ATCC 42981, we tested the strains in SM medium supplied with or without 2.0 M NaCl. This salt concentration was chosen because it was previously demonstrated to be the highest salt amount tolerated by all these yeasts (Solieri, Dakal and Bicciato 2014). Under standard conditions, allodiploid strain ATCC 42981 outcompetes *Z. sapae* ABT301^T and *Z. rouxii* CBS 732^T strains in growth performance (Fig. S1, panel A Supporting Information). The data presented herein are congruent with the previously reported phenotypic profiling (Solieri, Dakal and Bicciato 2014), and reflect an increase in growth fitness frequently observed for allodiploids (Chen 2013). When cultured in NaCl-SM medium, ATCC 42981 adapted to salt-stress conditions better than *Z. sapae* and *Z. rouxii* (Fig. S1, panel B Supporting Information). However, we observed strong reduction in growth performance for all the strains under hyperosmotic injury. In particular, salt stress reduces growth rate (μ) and inhibits the maximum cell growth (A). Unfortunately, the low biomass production makes difficult to recover appropriate cell amounts for subsequent polyol determination and RNA extraction for transcriptional studies.

Yeasts facing environmental cues display increased nutrient requirements compared to standard conditions, in order to sustain highly energy-consuming stress-related functions, such as production, accumulation and retention of metabolically compatible osmolytes (Broach 2012). Like nutrient starvation, high osmolarity elicits the repression of gene sets with growth-related functions, and redirects resources from proliferation to stress protection (Gasch *et al*. 2000). Several works demonstrated that nutrient limitation rather than inhibitor effects of stressor is responsible for the inability of yeasts to survive stress conditions (López-Maury, Marguerat and Bähler 2009 and references therein). Besides carbon, nitrogen compounds have been recognised as key nutrients for yeast growth and proliferation, and, therefore, we investigated how *Zygosaccharomyces* yeasts respond to hyperosmotic stress under surplus availability of nitrogen sources. In particular, YE contains abundance of nitrogen, amino acid, vitamins and minor elements, and is usually used as source of growth stimulants or growth factors for bacteria and yeasts. Figure 1 depicts growth curves of *Z. rouxii* CBS 732^T on SM, NaCl-SM, YESM and NaCl-YESM media, respectively. Visual inspection of growth curves demonstrated that CBS 732^T grows faster when YNB was supplemented with YE (NaCl-YESM) as compared to NaCl-SM medium. As NaCl-YESM and NaCl-SM media contain the same amount of stressor, we speculated that YE supplementation uncouples surplus of energy demand from salt toxic effects. Similarly, the salt-tolerant yeast *Hortaea werneckii* get benefits from the supplementation of additional nitrogen sources which allows the cells to better sustain the demand of additional energy under salt stress (Vaupotič and Plemenitaš 2007). Based on this evidence, we selected NaCl-YESM as medium for testing differences in growth performance of *Zygosaccharomyces* strains in response to salt stress.

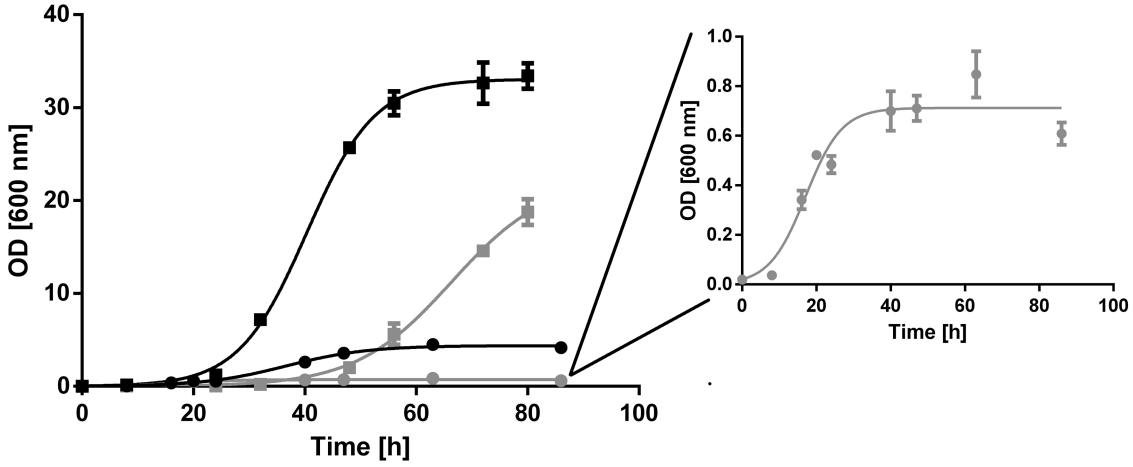

Figure 1. Effect of nitrogen supplementation on growth behaviour of *Z. rouxii* CBS 732T. Growth was measured over time as OD at 600 nm in four different media (SM, black circles; NaCl-SM, grey circles; YESM, black squares; and NaCl-YESM, grey squares). OD values are means of three independent replicas and bars (when appreciable) represent standard deviation (SD) values. Top bottom zoom represents growth curve in NaCl-SM. All growth curves are fitted by the logistic model.

Growth assays

To determine relevant growth variables in YESM and NaCl-YESM media, like time to adapt to environmental challenge (λ), growth rate (μ) and efficiency of proliferation (A), we fitted the growth curves with three parametric models, such as Gompertz, logistic and Richards functions. The Richards model was discarded as being unable to fit the data (data not shown) and the best-fitting model was chosen between logistic and Gompertz equation models on the basis of AIC depending on specific combinations of strain and environmental conditions (Table S1, Supporting Information). The resulting complete survey of growth parameters is listed in Table 2.

Growth comparison in YESM medium confirmed significant interstrain differences in control conditions, as previously reported (Solieri, Dakal and Bicciato 2014). In particular, allodiploid strain ATCC 42981 displayed a fast-growing behaviour with shorter lag phase, higher growth rate and greater biomass accumulation at stationary phase than *Z. sapae* ABT301^T ($P < 0.001$) (Table 2). Remarkably, μ and A parameters suggest that, under surplus of nitrogen source and in absence of salt, *Z. rouxii* CBS 732^T overcame ATCC 42981 in growth performance ($P < 0.001$). This result partially disagrees with that found in nitrogen-deficient medium (Solieri, Dakal and Bicciato 2014), where CBS 732^T displayed the intermediate basal phenotype between the fast-growing ATCC 42981 and the low-growing ABT301^T. So we inferred that nitrogen supplementation probably complements some growth defects in strain CBS 732^T.

The supplementation with YE also changed significantly the salt-stress response (Table 2). Comparison of growth parameters between YESM and NaCl-YESM media shows that all strains suffered growth defects with respect to all growth variables. The difference in the latency time in case of ATCC 42981 was registered shortest suggesting that ATCC 42981 does not require time to adapt to salt stress. Furthermore, ATCC 42981 exhibited a slight reduction of μ and A parameters in salt compared to basal conditions (Table 2). Contrastingly, under salt stress CBS 732^T markedly reduced μ and A parameters and delayed the onset of growth by approximately 22.4 h. This delay can be attributed to gradual and time-consuming adaptation of the cells to the high salt concentration, but it might also be due (at least partially) to the propagation of tolerant subpopulations which might have been present as a minor component in the inoculum. Stratford *et al.* (2014) demonstrated that in *Z. bailii*, a relative of *Z. rouxii* species complex, ascorbic acid sensitive subpopulations are replaced by the resistant subpopulations, leading to a significant increase in lag phase. Despite this delay, CBS 732^T outplayed ATCC 42981 and ABT301^T in maximum growth rate and efficiency of proliferation. Together, these data indicate that, even though CBS 732^T displays higher growth fitness in nitrogen-rich medium supplemented with NaCl, it requires more time to adapt to this environmental perturbation and shows decreased growth rate and efficiency of proliferation at a greater extent than ATCC 42981. Therefore, when the growth parameters in salt were normalised with respect to growth behaviour in control conditions, ATCC 42981 was found to be the most salt-tolerant strain within the *Z. rouxii* complex in nitrogen-rich conditions too.

Glycerol production and retention

Glycerol is usually synthesised by cells upon high external NaCl concentrations to counteract water outflow (van Zyl, Kilian and Prior 1990; Lages, Silva-Graca and Lucas 1999). However, the synthesised glycerol may be partially leaked by diffusion through the plasma membrane. It is generally reported that high salt-tolerant yeasts differ from less salt-tolerant ones in their ability to better counteract the glycerol diffusion and accumulate it into cytosol. In order to examine the role of glycerol in *Zygosaccharomyces* salt response, intra- and extracellular glycerol contents were determined in salt-stressed and unstressed cells recovered at L and S phases.

As shown in Fig. 2, strain ATCC 42981 grown in standard conditions exhibited higher extracellular glycerol content than ABT301^T and CBS 732^T in both growth phases L and S. Glycerol was highly extruded into the surrounding medium by exponentially growing cells of ATCC 42981, reaching 1.42 ± 0.09 μmol/10^7 CFU, than declined to 0.91 ± 0.03 μmol/10^7 CFU at the stationary phase. Under salt stress ATCC 42981 reported 3- to 5-fold increased intracellular glycerol compared to control conditions. L-growing ATCC 42981 cells intracellularly accumulated glycerol in response to salt better than ABT301^T and CBS 732^T (Fig. 2). In contrast, when cells reached the stationary phase, no significant differences were detected among strains in intracellular glycerol. The increased ability of ATCC 42981 to accumulate glycerol intracellularly in response to salt could rely on the reduction of membrane permeability to glycerol or on the shift of metabolic flux towards glycerol biosynthesis. However, we did not detected any statistical difference in total glycerol production (sum of intra- and extracellular amounts) between unstressed and salt-stressed ATCC 42981 cells grown to the exponential phase (1.30 ± 0.11 vs 1.59 ± 0.07 μmol/10^7 CFU; $P = 0.0615$). This finding suggests that ATCC 42981 exhibits a strong basal

Table 2. Growth trait variation induced by 2 M NaCl in *Z. rouxii* complex yeasts. Growth assays in YESM (control) and NaCl-YESM (2 M NaCl) media were carried out by three biological replicates. The uncertainty-normalised differences (σ) are statistically different when $|\sigma| > 3$. σ values computed for each pairwise comparison between strains under the same environmental condition are reported in Table S2 (Supporting Information).

				Growth parameters(±SE)								
Strains	Conditions	Best-fitting model	R square	λ (h)	$\lvert\sigma\rvert$	$\lvert\Delta\lambda\rvert$	μ (h^{-1})	$\lvert\sigma\rvert$	$\lvert\Delta\mu\rvert$	A	$\lvert\sigma\rvert$	$\lvert\Delta A\rvert$
ABT301^T	Control	Gompertz	0.98	30.36 ± 1.51	17.55	30.15	0.50 ± 0.03	3.33	0.12	25.26 ± 1.01	13.27	13.69
	2 M NaCl	Logistic	0.99	60.51 ± 0.82			0.38 ± 0.02			11.57 ± 0.21		
CBS 732^T	Control	Gompertz	0.99	26.72 ± 0.56	21.64	22.39	1.35 ± 0.06	10.43	0.70	33.58 ± 0.45	7.10	11.12
	2 M NaCl	Logistic	0.98	49.11 ± 0.87			0.65 ± 0.02			22.46 ± 1.50		
ATCC 42981	Control	Gompertz	0.98	22.52 ± 0.89	3.27	4.84	0.72 ± 0.04	5.00	0.26	22.05 ± 0.46	12	7.17
	2 M NaCl	Logistic	0.99	27.36 ± 1.18			0.46 ± 0.03			14.88 ± 0.31		

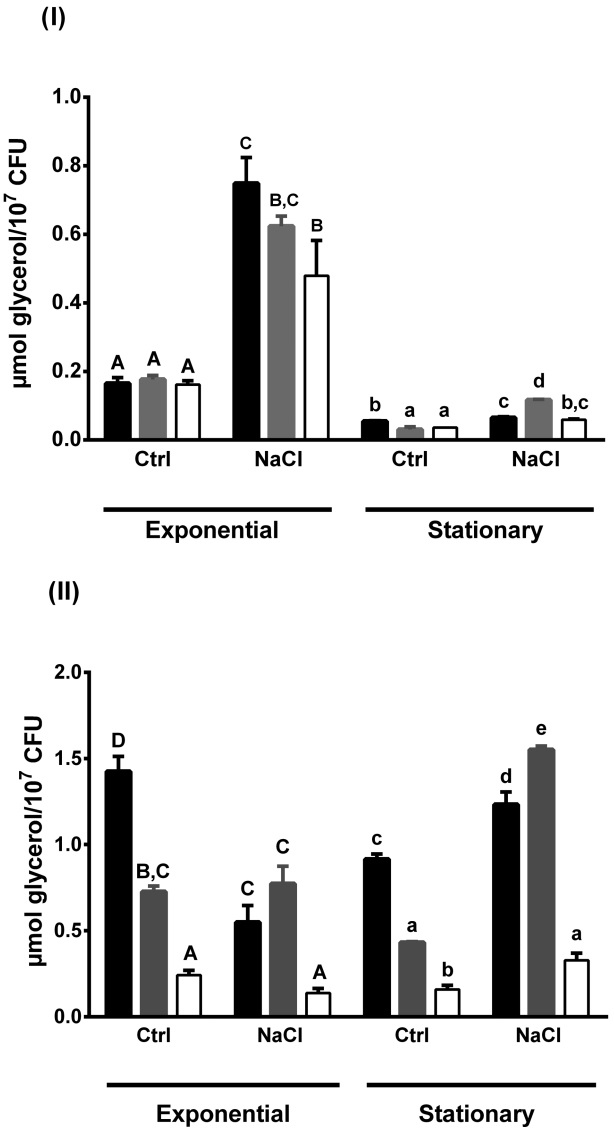

Figure 2. Impact of salt stress on glycerol content. Temporal changes of intracellular (I) and extracellular (II) glycerol concentrations (expressed as μmol/107 CFU) are reported for allodiploid ATCC 42981 (black), *Z. sapae* ABT301T (grey) and *Z. rouxii* CBS 732T (white) cells grown under control (Ctrl) and 2 M NaCl conditions and sampled at exponential and stationary phases, respectively. Values represent means ± SD ($n = 3$); bars with different uppercase (exponential phase) and lowercase (stationary phase) letters are statistically significant (two-way ANOVA and Tukey's multiple comparison tests; $P < 0.05$).

glycerol production and responds to salt by enhancing glycerol retention inside the cell without any significant increase of glycerol biosynthesis.

Under standard conditions, L-growing cells of *Z. sapae* ABT301^T mainly extruded glycerol into the surrounding medium, but the level of extracellular glycerol was significantly lower than that observed for ATCC 42981 (Fig. 2). Under salt stress, *Z. sapae* grown to exponential phase increased both total glycerol production (1.39 ± 0.10 vs 0.90 ± 0.02 μmol/10^7 CFU; $P = 0.0143$) and intracellular glycerol retention compared to unstressed cells (Fig. 2). As result, strain ABT301^T intracellularly accumulated more glycerol in response to salt than *Z. rouxii* CBS 732^T, but less than ATCC 42981. At the stationary phase, ABT301^T stressed cells synthesised higher amount of glycerol (sum of intra- and extracellular glycerol) than unstressed cells ($P = 0.0002$). ABT301^T extracellularly released this additional glycerol amount to significantly greater extent than ATCC 42981.

Like *Z. sapae* ABT301^T, L-growing cells of *Z. rouxii* CBS 732^T slightly increased the overall glycerol production in response to salt and mainly retained this glycerol surplus at intracellular level. However, glycerol production and retention were significantly lower than those detected in strains ATCC 42981 and ABT301^T (Fig. 2).

Overall these pieces of evidence support that ATCC 42981 has a better cellular system to accumulate glycerol compared to *Z. rouxii* CBS 732^T and *Z. sapae* ABT301^T. *Zygosaccharomyces rouxii* and *Z. sapae* exhibit a low basal glycerol production and need to spend energy to *de novo* synthesise glycerol under salt stress. In contrast, ATCC 42981 has a 'fast' strategy to adapt to hyperosmotic stress: it constitutively produces high glycerol amount and responds to salt stress by reducing the glycerol leakage.

Glycerol production and retention upon hyperosmotic stress is mediated by the HOG MAPK signalling cascade, which enhances glycerol synthesis, induces the closure of the facilitated diffusion channel Fps1 and positively regulates the expression of active glycerol importer Stl1 (Dakal, Solieri and Giudici 2014 and references herein). A possible explanation accounting for the different glycerol balance applied by the *Zygosaccharomyces* yeasts in osmotically non-optimal environments could entail glycerol biosynthesis and glycerol-import capacity. Allodiploid ATCC 42981 genome has two genes encoding MAP kinase Hog1 (*ZrHOG1* and *ZrHOG2*), two genes encoding glycerol dehydrogenase (*ZrGCY1* and *ZrGCY2*) and two genes encoding glycerol 3-phosphate dehydrogenase (*ZrGPD1* and *ZrGPD2*). Differently from ATCC 42981, CBS 732^T possesses only one homologous gene for *ZrHOG1* and *ZrHOG2* (ZYRO0D06182g), *ZrGCY1* and *ZrGCY2* (ZYRO0F10032g) and *ZrGPD1* and *ZrGPD2* (ZYRO0A05390g). Both *ZrHOG1* and *ZrHOG2* genes are significant in either osmotic regulation or ion homeostasis (Iwaki, Tamai and Watanabe 1999). ATCC 42981 constitutively expresses *ZrGPD1* and *ZrGPD2* genes. ZrGpd1 and ZrGpd2 proteins belong to the Gpd-Gpp glycerol pathway, that includes the conversion of dihydroxyacetone phosphate (DHAP) to glycerol 3-phosphate mediated by glycerol-3-phosphate dehydrogenase (Gpd), and the subsequent dephosphorylation of glycerol 3-phosphate to glycerol by glycerol-3-phosphatase enzyme (Gpp) (Iwaki *et al.* 2001). Therefore, this pathway could account for the high basal production of glycerol observed for ATCC 42981. In contrast, the moderately salt-tolerant *Saccharomyces cerevisiae* mainly increases glycerol production in response to osmotic stimuli via the Gpd-Gpp glycerol pathway (Dakal, Solieri and Giudici 2014). Furthermore, Iwaki *et al.* (2001) demonstrated that transcripts of *ZrGCY1* and *ZrGCY2* genes increased in salt-stressed ATCC 42981 cells compared to unstressed ones, suggesting that salt elicits the so-called Gcy-Dak pathway, which includes the oxidation of glycerol to dihydroxyacetone (DHA) catalysed by glycerol dehydrogenase (Gcy) and the phosphorylation of DHA to DHAP by dihydroxyacetone phosphate kinase (Dak). This pathway is involved in stress adaptation, but its role is not clearly understood. Interestingly, the salt induction of the *ZrGCY* gene transcription in ATCC 42981 suggests that the Gcy-Dak pathway for dissimilation of glycerol also get activated under salt-stress condition (Iwaki *et al.* 2001). However, to what extent this assumption is true has not be deciphered until yet. If Gcy1 and Gcy2 get induced under salt-stress condition, there should be apparent reduction in glycerol amount in ATCC 42981. However, in the current study, we did not record any change in the total glycerol content in the stressed and unstressed cells during

L phase. Furthermore, the entire pathway of glycerol conversion to DHAP requires one ATP molecule, an energy-consuming scenario quite unrealistic to occur under stress condition. In this perspective, Watanabe, Tsuchimoto and Tamai (2004) previously demonstrated that heterologous expression of *ZrGCY1* in *S. cerevisiae* did not decrease the glycerol content, suggesting that increased *ZrGCY1* and *ZrGCY2* transcripts have a role other than glycerol dissimilation during stress response in ATCC 42981, such as redox balance (Costenoble *et al.* 2000), ATP pool balance (Blomberg 2000) and DHA detoxification (Molin, Norbeck and Anders Blomberg 2003).

Concerning the glycerol-import capacity, CBS 732^T was recently proven to possess two genes both encoding transporters mediating active glycerol uptake, namely *STL1* and *STL2* (Dušková *et al.* 2015a,b). As being allodiploid, ATCC 42981 could have additional *STL*-like genes, which may get involved in cell survival to saline stress and account for the high effectiveness in glycerol retention observed at exponential phase.

Mannitol production and retention

Mannitol is known to be produced in response to osmotic stress by halotolerant species belonging to the genera *Debaryomyces*, *Candida*, *Wickerhamomyces* and *Saccharomycopsis* (Dakal, Solieri and Giudici 2014). To establish whether *Zygosaccharomyces* strains also produce mannitol as compatible osmolyte under hypersaline conditions, we determined intra- and extracellular mannitol content in cells grown to exponential and stationary phases. Figure 3 shows that all strains produced low mannitol levels under any condition tested, and generally released mannitol into the surrounding medium. Under standard conditions, ATCC 42981 is the best mannitol-producer strain mainly at exponential phase. In response to salt stress, all strains down-regulated mannitol production. These results suggest that salt-mediated osmotic pressure does not induce mannitol production, and are largely consistent with the previous observations that mannitol is mainly synthesised in response to high sugar rather than salt concentrations (Onishi and Suzuki 1968; Koganti *et al.* 2011).

Qualitative expression analysis of the *ZrSOD* genes

When extracellular cation concentration is higher than the physiological range, the cell requires activating different type of cation efflux systems for assuring adjustments of cellular pH, cell volume and membrane potential (Dakal, Solieri and Giudici 2014). As summarised in Table 1, *Z. rouxii* differs from *Z. sapae* and allodiploid strain ATCC 42981 in Na^+/H^+ antiporters-encoding *ZrSOD* gene variants (Watanabe, Miwa and Tamai 1995; Kinclová, Potier and Sychrová 2001; Solieri, Cassanelli and GiudicI 2007; Solieri *et al.* 2008). However, the transcriptional regulation of these genes in response to salt stimuli has been poorly studied. Therefore, we analysed the exponential-phase transcriptional profile of three Na^+/H^+ antiporter-encoding genes, namely *ZrSOD2*, *ZrSOD2-22* and *ZrSOD22* in response to salt. RT-PCR assays showed that L- and S-grown CBS 732^T cells transcribed *ZrSOD2-22* gene in both basal and salt conditions (data not shown). Both *ZrSOD22* and *ZrSOD2* gene copies are constitutively transcribed by salt-stressed and unstressed cells of ATCC 42981 in exponential growth phase (Fig. S2, panel A Supporting Information). *SOD2-22* and *SOD22* genes were also transcribed by NaCl-stressed and unstressed ABT301^T cells (Fig. S2, panel B). A similar result was found for all the strains grown to the stationary phase (data not shown). These findings partially disagree

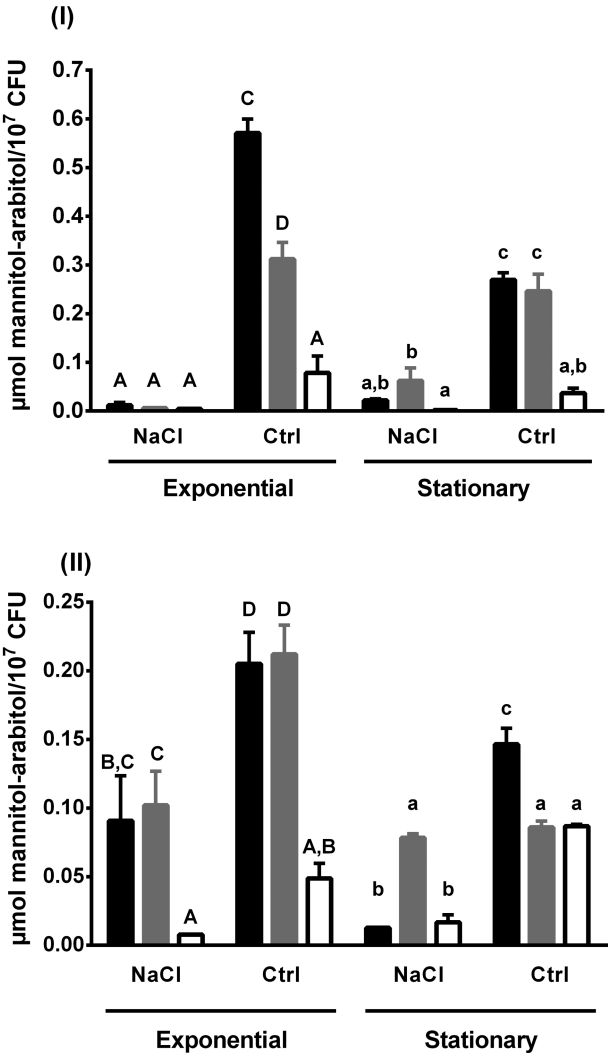

Figure 3. Impact of salt stress on mannitol content. Temporal changes of intracellular (I) and extracellular (II) mannitol concentrations (expressed as μmol/107 CFU) are reported for allodiploid ATCC 42981 (black), *Z. sapae* ABT301T (grey) and *Z. rouxii* CBS 732T (white) cells grown under control (Ctrl) and 2 M NaCl conditions and sampled at exponential and stationary phases, respectively. Values represent means ± SD ($n = 3$); bars with different uppercase (exponential phase) and lowercase (stationary phase) letters are statistically significant (two-way ANOVA and Tukey's multiple comparison tests; $P < 0.05$).

with an earlier study on ATCC 42981 (Iwaki *et al.* 1998). These authors reported that *ZrSOD22* gene transcription is inhibited by salt and concluded that *ZrSOD22* could be a pseudogene without any function in salt response or that it underwent functional divergence compared to the paralogous genes *ZrSOD2-22* and *ZrSOD22*. However, complementation experiment of *ZrSOD22* gene in *S. cerevisiae* salt-sensitive mutants showed that cells expressing *ZrSOD22* gene under a *S. cerevisiae* promoter control restore salt-tolerance immediately after exposure to NaCl (Iwaki *et al.* 1998). Conservation of 12 hydrophobic transmembrane domains and of the hydrophilic C-terminus between *ZrSOD2* and *ZrSOD2-22* also supports that they could have similar functions.

RT-qPCR primer validation

To further study these discrepancies and determine whether salt induces transcriptional modulation of Na^+/H^+ antiporters-

Figure 4. Primer location for *ZrSOD*-targeted RT-qPCR assays. Primer sets used to detect the *ZrSOD2-22*/*ZrSOD2* and *ZrSOD22* copy variants are boxed in blue and red, respectively. The sequences of *ZrSOD2-22* (GenBank accession number AJ252273), *ZrSOD2* (GenBank accession number D43629) and *ZrSOD22* (GenBank accession number AB010106) were aligned with Clustal Omega and the relative primer positions are indicated by arrows. Identical sites are illustrated by asterisks.

Table 3. Primer pairs designed in this study and amplification results obtained by conventional and quantitative PCRs. Copy variant specificity was tested by PCR and qPCR and corresponding successful and unsuccessful results are indicated with plus or minus and separated by slash, respectively. E_T indicates theoretical efficiency as predicted by pcrEfficiency web tool (Mallona, Weiss and Marcos 2011); length indicates amplicons size in bp. *SOD22* full-length template was the gel-purified PCR amplicon obtained from ATCC 42981 by using previously validated external primer pair (Kinclová, Potier and Sychrová 2001).

				Copy-variant specificity				
Target gene	Primer pair	E_T	Length (bp)	ABT301^T	ATCC 42981	CBS 732^T	NCYC 3042	*ZrSOD22* full-length PCR template
ZrSOD2-22/*ZrSOD2*	SOD2-22_F1/SOD2-22_R1	1.94	136	+/+	+/+	+/+	–/ –/	–/–
ZrSOD22	SOD22_F4/SOD22_R4	1.64	115	+/+	+/+	–/–	+/+	+/+

encoding genes in ATCC 42981 and ABT301^T, we ascertained the transcriptional change of *SOD2*/*SOD2-22* and *SOD22* genes in response to salt by RT-qPCR. For this purpose, we assayed for expression of *ZrSOD* copy variants by designing specific RT-qPCR assays that distinguish the *ZrSOD* transcripts based on the presence of polymorphic sites. In particular, two primer sets, namely SOD2-22_F1/SOD2-22_R1 and SOD22_F4/SOD22_R4, were designed to selectively discriminate between *ZrSOD2-22*/*ZrSOD2* and *ZrSOD22* gene transcripts (Fig. 4). Initially, the effectiveness and specificity of these primers was evaluated by conventional PCR. When gDNAs from strains CBS 732^T (*ZrSOD2-22* gene) and NCYC 3042 (*ZrSOD22* gene) were used as template, neither SOD2-22_F1/SOD2-22_R1 or SOD22_F4/SOD22_R4 primer pairs show any cross-reactions against non-targets copy variants. The primer pairs were further tested using the gel-purified ATCC 42981 *ZrSOD22* full-length amplicon obtained from strain with external primers (Kinclová, Potier and Sychrová 2001) as template. This nested-PCR approach confirmed that only SOD22_F4/SOD22_R4 primer set was able to selectively amplify *ZrSOD22* gene variant. The copy variant-specificity of both primer pairs was also confirmed by qPCR through the analyses of melting curves and by gel electrophoresis. The melting curves of *ZrSOD2-22*/*ZrSOD2* and *ZrSOD22* PCR products had average T_m values of 76.01 ± 0.24 and 77.30 ± 0.30°C (mean ± standard deviation; $n = 12$), respectively. No other products were detected from non-target templates, either with melting curves (data not shown) or after migration of the PCR product on agarose gel (Table 3).

For primer set SOD2-22_F1/SOD2-22_R1, logarithmic-linear plots of ATCC 42981 and ABT301^T cDNAs concentrations vs C_T values generated slopes of –3.379 ± 0.08 ($r^2 = 0.99$; E = 97.67%) and –3.20 ± 0.10 ($r^2 = 0.99$; E = 105.4%), respectively. According to MIQE guidelines (Bustin *et al.* 2009), in both cases thresholds for the *ZrACT1* calibration curves were set up to gain comparable PCR efficiency values. In contrast, the optimization of the standard curve was unsuccessful for the gene target *ZrSOD22* and the LinReg method (Ruijter *et al.* 2009) was used as alternative to the standard gold method $2^{-\Delta\Delta Ct}$ (data not shown).

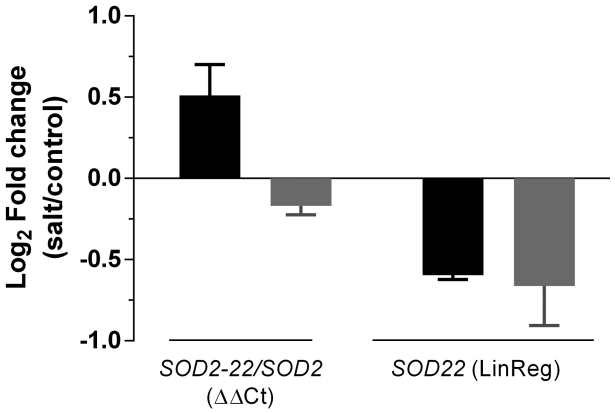

Figure 5. Differential expression of *ZrSOD* gene variants measured by RT-qPCR in ATCC 42981 and ABT301T cells after hyperosmotic stress. Histograms depict logarithmic expression changes (fold up- or downregulations) between stressed and unstressed cells of ABT301T (grey) and ATCC 42981 (black) grown to exponential phase. Expression of target genes was normalised on the reference gene ZrACT1 (GenBank: XM002497273). Fold change was measured by ΔΔCt or LinReg methods and reported as the mean (± SEM) of three biological replicates.

Quantitative gene expression of *ZrSOD* genes in response to salt stress

The RT-qPCR assays were used to quantify the differential mRNA expression of *ZrSOD* gene variants in ATCC 42982 and ABT301^T NaCl-stressed cells in exponential phase. As shown in Fig. 5, *Z. sapae* ABT301^T showed a slight 1.2-fold downregulation of *ZrSOD2-22* transcripts under hyperosmotic stress compared to control conditions. Conversely, allodiploid strain ATCC 42981 responded to salt by slightly upregulating *ZrSOD2* transcript. In both strains, *ZrSOD22* expression was slightly downregulated by salt. By applying a 2-fold change cut-off, no *ZrSOD* gene variants showed significant differences in mRNA expression (Fig. 5). These results indicate that Na^+/H^+ antiporter-encoding gene transcription is constitutive and salt independent both in ATCC 42981 and ABT301^T strains. Furthermore, the data suggest that differential regulation of *ZrSOD* genes does not occur and cannot be correlated with the phenotypic differences observed between ATCC 42981 and *Z. sapae* in salt tolerance. These findings are in line with those obtained by RT-PCR and congruent with the transcriptional profiling of the orthologous gene *NHA1* in model yeast *S. cerevisiae* (Ruiz and Ariño 2007). Like *ZrSOD* genes, *NHA1* does not undergo transcriptional changes in response to hyperosmotic injury. HOG pathway effectors modulate Nha1 activity at the plasma membrane by post-transcriptional modifications which determine the short-term response to salt (Proft and Struhl 2004). Similarly, ZrSod2-22, ZrSod2 and ZrSod22 antiporters could be post-transcriptionally regulated in *Zygosaccharomyces* yeasts under hyperosmotic stress to ensure a fast and acute response to salt.

The incongruence between our findings and previous results obtained by northern blotting (Iwaki *et al.* 1998) could be related to interlaboratory differences in growth conditions and recovery time. However, growth media were similar in both experiments (rich medium supplemented with yeast extract and 2 M NaCl), while recovery time was different. Iwaki *et al.* (1998) exposed ATCC 42981 cells to 2 M NaCl for a time interval ranging from 1 to 24 h, while in our experiments cells were grown to exponential phase (exposition time to salt ≥ 24 h). So, at present, we cannot rule out a delayed induction of *ZrSOD22* gene expression that might be silenced in ATCC 42981 cells immediately after exposition to NaCl shock and restored during exponential phase, when cells are well adapted to grow on hypersaline medium. Similarly in *S. cerevisiae* the transcriptional profile after saline stress depends on the timing of the response since it affects the set of responsive genes and the magnitude of their expression changes (Posas *et al.* 2000). A second possibility not mutually exclusive to the adaptive response relies on the population-level heterogeneity in *ZrSOD22* gene expression. The active transcription of *ZrSOD22* gene uncovered in exponentially growing cells cultured in hypersaline medium could be a clue for replacement of the bulk population by a slow-growing and salt-resistant subpopulation which actively transcribes *ZrSOD22* variant.

CONCLUSIONS

Understanding the molecular background of salt response in halotolerant yeasts is crucial to prevent yeast spoilage in salty food, to carry out fermentation of salt raw material under controlled conditions and to engine the halotolerant genes from yeast to other industrially relevant organisms. This work represents a first comparative attempt to unravel the cellular mechanisms responsible for the remarkable variation in stress response among the *Z. rouxii* complex yeasts. We show that *Z. rouxii*, *Z. sapae* and allodiploid ATCC 42981 have distinct behaviours after exposure to high extracellular Na^+ levels. In particular, ATCC 42981 exploits a 'low-cost' and pre-adaptive strategy to handle glycerol accumulation under high osmotic pressure, which depends on the effective enhance of intracellular glycerol retention rather than the increase of glycerol biosynthesis. *Zygosaccharomyces rouxii* and *Z. sapae* behaviour is instead strongly dependent on *de novo* glycerol biosynthesis and leads to extension of latency phase and strong reduction of proliferation efficiency. Differently from glycerol production, we found that *Z. sapae* and allodiploid ATCC 42981 have a similar transcriptional modulation of Na^+ extrusion systems during salt-induced stress. Two qPCR assays specific for *ZrSOD* gene variants demonstrate that both strains do not change their *ZrSOD* transcript levels after salt exposure, indicating that these Na^+-specific antiporters are transcriptionally unresponsive to salt. Taken all together, our data point future experiments towards the post-transcriptional modifications of ZrSod transporters and the study of effector molecules mediating intracellular glycerol accumulation as proximal causes behind halotolerance variation in the *Z. rouxii* complex.

SUPPLEMENTARY DATA

Supplementary data are available at FEMSYR online.

ACKNOWLEDGEMENTS

We acknowledge Luciana de Vero PhD for managing database of the Unimore Microbial Culture Collection (www.umcc.unimore.it).

FUNDING

The present work was supported by financial contributions from AEB Spa, Italy.

Conflict of interest. None declared.

REFERENCES

Bizzarri M, Giudici P, Cassanelli S *et al*. Chimeric sex-determining chromosomal regions and dysregulation of cell-type identity in a sterile *Zygosaccharomyces* allodiploid yeast. *PLoS One* 2016;**11**:e0152558.

Blomberg A. Metabolic surprises in *Saccharomyces cerevisiae* during adaptation to saline conditions: questions, some answers and a model. *FEMS Microbiol Lett* 2000;**182**:1–8.

Broach JR. Nutritional control of growth and development in yeast. *Genetics* 2012;**192**:73–105.

Bubnová M, Zemančíková J, Sychrová H. Osmotolerant yeast species differ in basic physiological parameters and in tolerance of non-osmotic stresses. *Yeast* 2014;**31**:309–21.

Bustin SA, Benes V, Garson JA *et al*. The MIQE guidelines: minimum information for publication of quantitative real-time PCR experiments. *Clin Chem* 2009;**55**:611–22.

Chen ZJ. Genomic and epigenetic insights into the molecular bases of heterosis. *Nat Rev Genet* 2013;**14**:471–82.

Costenoble R, Valadi H, Gustafsson L *et al*. Microaerobic glycerol formation in *Saccharomyces cerevisiae*. *Yeast* 2000;**16**:1483–95.

Dakal TC, Solieri L, Giudici P. Adaptive response and tolerance to sugar and salt stress in the food yeast *Zygosaccharomyces rouxii*. *Int J Food Microbiol* 2014;**185**:140–57.

De Nadal E, Ammerer G, Posas F. Controlling gene expression in response to stress. *Nat Rev* 2011;**12**:833–45.

Dušková M, Borovikova D, Herynkova P *et al*. The role of glycerol transporters in yeast cells in various physiological and stress conditions. *FEMS Microbiol Lett* 2015a;**362**:1–8.

Dušková M, Ferreira C, Lucas C *et al*. Two glycerol uptake systems contribute to the high osmotolerance of *Zygosaccharomyces rouxii*. *Mol Microbiol* 2015b;**97**:541–59.

Fleet GH. Yeast spoilage of food and spoilage. In: Kurtzman C, Fell J, Boekhout T *et al*. (eds). *The Yeast: A Taxonomic Study*, **vol**. **1**. Amsterdam: Elsevier Science, 2011, 53–63.

Gasch AP, Spellman PT, Kao CM *et al*. Genomic expression programs in the response of yeast cells to environmental changes. *Mol Biol Cell* 2000;**11**:4241–57.

Gordon JL, Wolfe KH. Recent allopolyploid origin of *Zygosaccharomyces rouxii* strain ATCC 42981. *Yeast* 2008;**25**:449–56.

Goujon M, McWilliam H, Li W *et al*. A new bioinformatics analysis tools framework at EMBL-EBI. *Nucleic Acids Res* 2010;**38**: W695–9.

Iwaki T, Higashida Y, Tsuji H *et al*. Characterization of a second gene (*ZSOD22*) of Na^+/H^+ antiporter from salt-tolerant yeast *Zygosaccharomyces rouxii* and functional expression of *ZSOD2* and *ZSOD22* in *Saccharomyces cerevisiae*. *Yeast* 1998;**14**: 1167–74.

Iwaki T, Kurono S, Yokose Y *et al*. Cloning of glycerol-3-phosphate dehydrogenase genes (*ZrGPD1* and *ZrGPD2*) and glycerol dehydrogenase genes (*ZrGCY1* and *ZrGCY2*) from the salt- tolerant yeast *Zygosaccharomyces rouxii*. *Yeast* 2001;**18**:737–44.

Iwaki T, Tamai Y, Watanabe Y. Two putative MAP kinase genes, *ZrHOG1* and *ZrHOG2* cloned from the salt-tolerant yeast *Zygosaccharomyces rouxii* are functionally homologous to the *Saccharomyces cerevisiae HOG1* gene. *Microbiology* 1999;**145**:241–8.

James SA, Bond CJ, Stratford M *et al*. Molecular evidence for the existence of natural hybrids in the genus *Zygosaccharomyces*. *FEMS Yeast Res* 2005;**5**:747–55.

Kinclová O, Potier S, Sychrová H. The *Zygosaccharomyces rouxii* strain CBS732 contains only one copy of the *HOG1* and the *SOD2* genes. *J Biotechnol* 2001;**88**:151–8.

Kinclová O, Potier S, Sychrová H. Difference in substrate specificity divides the yeast alkali-metal-cation/H^+ antiporters into two subfamilies. *Microbiology* 2002;**148**:1225–32.

Kinclová-Zimmermannova O, Sychrová H. Functional study of the Nha1p C-terminus: involvement in cell response to changes in external osmolarity. *Curr Genet* 2006;**49**:229–36.

Koganti S, Min Kuo T, Kurtzman CP *et al*. Production of arabitol from glycerol: strain screening and study of factors affecting production yield. *Appl Microbiol Biot* 2011;**90**:257–67.

Lages F, Silva-Graca M, Lucas C. Active glycerol uptake is a mechanism underlying halotolerance in yeasts: a study of 42 species. *Microbiology* 1999;**145**:2577–85.

Livak KJ, Schmittgen TD. Analysis of relative gene expression data using real-time quantitative PCR and the $2^{-ddC(T)}$ Method. *Methods* 2001;**25**:402–8.

López-Maury L, Marguerat S, Bähler J. Tuning gene expression to changing environments: from rapid responses to evolutionary adaptation. *Nat Rev Genet* 2009;**9**:583–93.

Mallona I, Weiss J, Marcos E-C. pcrEfficiency: a web tool for PCR amplification efficiency prediction. *BMC Bioinformatics* 2011;**12**:404–11.

Molin M, Norbeck J, Anders Blomberg A. Dihydroxyacetone kinases in *Saccharomyces cerevisiae* are involved in detoxification of dihydroxyacetone. *J Biol Chem* 2003;**278**:1415–23.

Onishi H, Suzuki T. Production of D-mannitol and glycerol by yeasts. *Appl Microbiol* 1968;**16**:1847–52.

Posas F, Chambers JR, Heyman JA *et al*. The transcriptional response of yeast to saline stress. *J Biol Chem* 2000;**275**: 17249–55.

Proft M, Struhl K. MAP kinase-mediated stress relief that precedes and regulates the timing of transcriptional induction. *Cell* 2004;**118**:351–61.

Ruijter JM, Ramakers C, Hoogaars WM *et al*. Amplification efficiency: linking baseline and bias in the analysis of quantitative PCR data. *Nucleic Acids Res* 2009;**37**:e45.

Ruiz A, Ariño J. Function and regulation of the *Saccharomyces cerevisiae ENA* sodium ATPase system. *Eukaryote Cell* 2007;**6**: 2175–83

Solieri L, Cassanelli S, Croce MA *et al*. Genome size and ploidy level: new insights for elucidating relationships in *Zygosaccharomyces* species. *Fungal Genet Biol* 2008;**45**:1582–90.

Solieri L, Cassanelli S, GiudicI P. A new putative *Zygosaccharomyces* yeast species isolated from traditional balsamic vinegar. *Yeast* 2007;**24**:403–17.

Solieri L, Dakal TC, Bicciato S. Quantitative analysis of multistress response in *Zygosaccharomyces rouxii* complex. *FEMS Yeast Res* 2014;**10**:1364–12146.

Solieri L, Dakal TC, Croce MA *et al*. Unravelling genomic diversity *of Zygosaccharomyces rouxii* complex with a link to its life cycle. *FEMS Yeast Res* 2013;**13**:245–58.

Solieri L, Dakal TC, Giudici P. *Zygosaccharomyces sapae* sp. nov., a novel yeast species isolated from Italian traditional balsamic vinegar. *Int J Syst Evol Micr* 2013;**63**:364–71.

Solieri L, Giudici P. Yeasts associated to traditional balsamic vinegar: ecological and technological features. *Int J Food Microbiol* 2008;**125**:36–45.

Stratford M, Steels H, Nebe-von-Caron G *et al*. Population heterogeneity and dynamics in starter culture and lag phase adaptation of the spoilage yeast Zygosaccharomyces bailii to weak acid preservatives. *Int J Food Microbiol* 2014;**181**: 40–7.

Stratford M. Food and beverage spoilage yeasts. In: Querol A, Fleet GH (eds). *Yeasts in Food and Beverages*. Berlin: Springer, 2006, 335–80.

Suezawa Y, Suzuki M, Mori H. Genotyping of a miso and soy sauce fermentation yeast, *Zygosaccharomyces rouxii*, based on sequence analysis of the partial 26S ribosomal RNA gene and two internal transcribed spacers. *Biosci Biotech Bioch* 2008;**72**:2452–5.

van Zyl PJ, Kilian SG, Prior BA. The role of an active transport mechanism in glycerol accumulation during osmoregulation by *Zygosaccharomyces rouxii*. *Appl Microbiol Biot* 1990;**34**:231–5.

Vaupotič T, Plemenitaš A. Differential gene expression and Hog1 interaction with osmoresponsive genes in the extremely halotolerant black yeast *Hortaea werneckii*. *BMC Genomics* 2007;**8**:280.

Watanabe Y, Miwa S, Tamai Y. Characterization of Na^+/H^+-antiporter gene closely related to the salt-tolerance of yeast *Zygosaccharomyces rouxii*. *Yeast* 1995;**11**:829–38.

Watanabe Y, Tsuchimoto S, Tamai Y. Heterologous expression of *Zygosaccharomyces rouxii* glycerol 3-phosphate dehydrogenase gene (*ZrGPD1*) and glycerol dehydrogenase gene (*ZrGCY1*) in *Saccharomyces cerevisiae*. *FEMS Yeast Res* 2004;**4**:505–10.